Title: Single cell analysis reveals the molecular signaling and cellular composition of the regenerating *Hydra* head

Authors: Aide Macias-Muñoz[1,2,*], Lisa Y. Mesrop[2], Heidi Yahan Liang[1], Ali Mortazavi[1,*]

[1] Department of Developmental and Cell Biology, University of California, Irvine, CA, 92697 U.S.A.

[2] Department of Ecology, Evolution, and Marine Biology, University of California Santa Barbara, CA, 93106 U.S.A.

*Corresponding authors: Ali Mortazavi, ali.mortazavi@uci.edu; Aide Macias-Muñoz, amaciasm@ucsb.edu

Key words: Wnt3, regeneration, head organizer, Jun, Fos, Sox

Abstract:

The extent to which animals can regenerate cells, tissues, or body parts varies largely. *Hydra* has a remarkable ability to undergo full body regeneration. Bisected polyps can regenerate the head and foot, and whole polyps can form from aggregates of cells. This capability is made possible by a cluster of cells known as the head organizer. This organizer has the capability to self-regulate and to induce a second axis. Previous studies have found *Wnt3* and other developmental genes associated with head organizer function. Yet, the cellular composition and molecular program of regenerating tissue remains largely unknown. In this study, we used single cell RNA-seq from a regeneration time course to identify the molecular and cellular features of *Hydra* head regeneration. We identified nine distinct cell types in the regenerating head tissue, including candidate head organizer cells. We found Wnt-signaling and early wound response genes co-expressed with *Wnt3*, and all were more highly expressed in the head organizer cell cluster. In addition, we found that *Wnt3* expression is likely being regulated by conserved developmental transcription factors. Our study reveals coordination of early wound response, developmental transcription factors, and transposable elements during *Hydra* tissue regeneration and provides insight into the evolution of development and regeneration programs.

Introduction

Tissue regeneration, which is the capacity to self-renew and differentiate into specific tissues, is a complex process involving the coordination of various cell types and genetic regulatory programs. The extent of regeneration in animals vary between organisms and tissue types, ranging from tissues with minimal regeneration capacities, such as mammalian heart and brain, to whole organism generation, such as in *Hydra (*. Trembley discovered in 1744 that *Hydra* is capable of fully regenerating parts of its body (. Its body consists of two tissue layers and a simple axial structure made up of the hypostome, tentacles, body column, and foot (Figure 1A). A bisected *Hydra* can regenerate its head and foot (. Adult polyps can be dissociated into cell aggregates that are capable of reforming a polyp (Noda, 1971; Technau et al., 2000). In 1909, Browne performed a variety of graft transplantations to identify the tissues necessary to induce ectopic head development and thus found the first evidence of a head organizer in *Hydra* (Browne, 1909). The *Hydra* head organizer is a cluster of endoderm and ectoderm cells at the tip of the hypostome, hypothesized to be anywhere from 5 to 180 epithelial cells, that is responsible for axial patterning and head regeneration (Bode, 2012; Gierer et al., 1972; Technau et al., 2000). Under normal circumstances, *Hydra* epithelial cells are constantly undergoing mitosis and being sloughed off at the foot, the tips if the tentacles, and the tip of the hypostome. Axial patterning is maintained by the head organizer with head activator and head inhibitor capacities that maintain a head and second axis (Broun and Bode, 2002). During regeneration, the head organizer forms within 8 hours after bisection (Bode, 2003). While regeneration in *Hydra* is a long-standing topic of investigation, there are still gaps in knowledge regarding the temporal dynamics and molecular basis of the head organizer.

Previous *in situ* hybridization and chemical inhibition studies, have identified various developmental genes and transcription factors (TFs) involved in the *Hydra* head organizer processes. Some of the most well studied genes in *Hydra* are members of the Wnt family, especially *Wnt3*. *Wnt3*, *β-catenin* and *Tcf* genes are expressed in the hypostome of the adult *Hydra* polyp, the regenerating head, and the hypostome of a developing polyp formed by budding (asexual reproduction) (Hobmayer et al., 2000; Nakamura et al., 2011a). *Wnt3* expression is controlled by two *cis*-regulatory elements that are directly influenced by Wnt/β-catenin signaling (Nakamura et al., 2011a). Other Wnt genes (*Wnt1*, *Wnt7*, *Wnt9/10a*, *Wnt9/10c*, *Wnt11* and *Wnt16*) are also expressed in the adult hypostome, during budding, and during regeneration (Lengfeld et al., 2009). These genes are expressed in both the endoderm and ectoderm of adult polyps, but their expression dynamics vary during budding and regeneration (Lengfeld et al., 2009). Homologs of the vertebrate axial patterning genes *Brachyury* and *Goosecoid* have also been associated with the head organizer. *Hydra Brachyury1 (HyBra1*) is expressed in the endoderm of the adult hypostome, during budding, and early during regeneration (~3 hours post bisection) (Bielen et al., 2007; Technau and Bode, 1999). *HyBra2*, on the other hand, is expressed in the ectoderm layer of the hypostome and appears later during regeneration (between 6 to 15 hours) (Bielen et al., 2007). *Hydra Goosecoid* (*Gsc*) is expressed in 3 locations in the *Hydra* body, two of which are in the head region and the third in the body column. *Gsc* is expressed in the hypostome ectoderm and in the endoderm at the tentacle base of adult *Hydra* (Broun et al., 1999). During budding and regeneration, *Gsc* expression appears early in the endoderm, then is found in the ectoderm at the tip of the new hypostome and in the endoderm as a ring where tentacles will form (Broun et al., 1999). Notch, another conserved developmental pathway, is also implicated in the head organizer.

Treatment of *Hydra* with DAPT, a Notch signaling inhibitor, results in malformed heads (Münder et al., 2013).

A candidate gene approach provided strong evidence and validation for the actions of conserved signaling molecules and TFs. Advances in sequencing technologies and generation of a *Hydra* genome then allowed us to identify additional candidate genes and TFs used by *Hydra* for head regeneration (Chapman et al., 2010; Steele, 2012). A proteomic and transcriptomic analysis identified two mechanisms for *Hydra* head regeneration (Petersen et al., 2015). First, *Hydra* undergoes a response to injury, followed by patterning. The injury response and wound closure is associated with cell cycle control, nucleic acid binding, cytokinesis, cell signaling, and novel *Hydra* proteins (Petersen et al., 2015). Regeneration and patterning, on the other hand, is associated with developmental signaling pathways such as Wnt, TGF beta, Jak/STAT, MAPK and mTOR (Petersen et al., 2015). A study using RNA-seq and ATAC-seq to compare head and foot regeneration in *Hydra* found differences in early injury response and later regeneration (Cazet et al., 2021). Injury response chromatin accessibility and gene expression is similar in head and foot and includes upregulation of Wnt genes and *HyBra1* (Cazet et al., 2021). Genes associated with regeneration after injury included *FoxM1*, *Fos*, and *Sox2* (Cazet et al., 2021). Another study used RNA-Seq, ATAC-Seq and ChIP-Seq to identify changes in gene expression and chromatin accessibility during regeneration (Murad et al., 2021). This study identified genes upregulated in the adult *Hydra* hypostome and during regeneration including Wnt genes, *KS1*, *aristaless related homeobox (HyAlx*), *Brachyury (Bra*), *COUP-TF*, and *orthodenticle homeobox* (*Otx*). Peaks with dynamic accessibility during regeneration were enriched for transcription factor binding sites (TFBS) including paired box (Pax), forkhead box (Fox), SRY-related HMG-box (Sox) and Goosecoid (Gsc). Moreover, ChIP-seq on an adult polyp with chemically activated Wnt/β-catenin

signaling using alsterpaullone showed an enrichment of H3K27ac for *Wnt5a*, *Wnt11*, *HyBra1*, *Gsc*, and *Pitx* (Reddy et al., 2020). These four studies provide a suite of additional genes and TFs that may be involved in the actions of the head organizer.

Recent advances in single cell RNAseq (scRNA-seq) technology and analysis software now allow for resolution at the single cell level. For model cnidarians, scRNA-seq has been used to describe cell types, genes specific to different cell types, and expression profiles of conserved developmental genes (Chari et al., 2021; Sebé-Pedrós et al., 2018; Siebert et al., 2019). In *Hydra*, scRNA-seq data from different developmental stages were clustered by cell linage (ie. endoderm, ectoderm, and interstitial) and cell types which included battery, stem, neuron, nematoblast, nematocyte, and gland cells (Siebert et al., 2019). In terms of regeneration, scRNA-seq was used to discover a newly described epidermis cell type that responds to injury and is responsible for wound healing in *Xenopus* (Aztekin et al., 2019). By contrast, scRNA-seq in axolotls uncovered that connective tissue cells with adult phenotype can revert to an embryo-like phenotype during regeneration (Gerber et al., 2018). These studies suggest that scRNA-seq can help us identify the *Hydra* head organizer cells and their molecular signaling.

Hydra is a member of the phylum Cnidaria, which is sister to Bilateria that consists of animals with bilateral symmetry. Several developmental genes are used for regeneration in cnidarians and early branching bilaterians of the Xenacoelomorpha and Platyhelminthes phyla. For example, *Wnt/β-catenin*, *Fox*, *Sox*, *Six*, and *Otx* genes function in regeneration in the planarian *Schmidtea mediterranea* and the anthozoan *Nematostella vectensis* (Schaffer et al., 2016). In the acoel *Hofstenia*, *Wnt3* signaling is necessary for posterior regeneration (Ramirez et al., 2020). Comparing the regeneration programs between Cnidaria and early branching Bilateria will tells us about conservation and variations in gene function and gene regulatory network connectivity.

In this study, we used scRNA-seq from the adult *Hydra* hypostome and during a time course of regeneration to determine the cell types and genes involved in *Hydra* head regeneration (Figure 1B). In addition, we used bulk RNA-seq and bulk ATAC-seq from a regeneration time course and hypostome (Murad et al., 2021) to determine gene expression modules and *cis*-regulation at the tissue level, respectively. We hypothesized that candidate regeneration genes would be co-expressed in regenerating tissue and in similar cell types. Using scRNA-seq, we identified 9 distinct cell types in regenerating tissues. *Wnt3*, the proposed marker of the head organizer, and most development transcription factors were predominantly expressed in head organizer and interstitial stem cells (i-cells). Using a weighted correlation network analysis (WGCNA) on bulk RNA-seq data, we identified a group of genes tightly co-expressed with *Wnt3*. Lastly, using pseudotime single cell trajectories for *Wnt3*-positive cell clusters and ATAC-seq data, we identified candidate *Wnt3* regulators. We provide a proposed model of *Hydra* head regeneration regulation and signaling based on previous literature and results from our analyses.

Results

Nine distinct cell types in regenerating Hydra head

Single cell RNA was collected from the *Hydra* adult hypostome and at three time points during head regeneration: 0, 4, and 12 hours post bisection (Figure 1B). Single cell RNA-seq libraries were sequenced to an average depth of ~80 million reads per library (Table S1). We recovered ~500-3,000 cells per sample after filtering (Table S1; Figure S1) for a total of 8626 cells. The cells grouped into 19 clusters (Figure S1). We determined cell types based on a *Hydra* single cell atlas (Siebert et al., 2019) using markers such as *KS1*, *Dkk1/2/4A*, *SoxC*, *nematogalectin*, *PaxA*, *mybX*, *KVamide*, and *Wnt3* (Figure S2). Based on these candidates for different cell types, we identified nine distinct cell types in the *Hydra* regenerating head: head epithelial endoderm

(4280 cells), head epithelial ectoderm (3386 cells), transposable element high (TE high; 104 cells), TE high with Wnt signaling (212 cells), interstitial stem (i-cell; 89 cells), nematoblast and cnidocyte (153 cells), neuron (325 cells), and head organizer cells (77 cells) (Figure 1C).

Transcript-level analysis

For increased resolution, we initially mapped reads to a reference transcriptome that contains transcript isoforms. Using transcripts rather than genes, cells grouped into nine clusters: clusters 0-8 (Figure S3). These clusters were defined by the most highly differentially expressed transcripts, which we refer to as top markers for cell types (Figure S4). We then analyzed the genes that harbor these transcripts and verified cell type identities by looking at the expression of these genes in a *Hydra* single cell atlas available at https://singlecell.broadinstitute.org/ (Siebert et al., 2019). The top markers for Clusters 0, 1, and 2 included *KS1*, *Antistasin, Dkk1/2/4A*, *PPOD1*, neuroblast differentiation-associated protein *AHNAK*, *chymotrypsin*, *zinc finger 862*, and transcription factor *BTF3* (Figure S5). *KS1* is highly expressed in the hypostome ectoderm (Endl et al., 1999; Murad et al., 2021; Weinziger et al., 1994). *Antistasin* genes are expressed in gland and mucous cells with higher expression in the *Hydra* head (Holstein et al., 1992; Wenger et al., 2016). *PPOD1* and *HyDkk1/2/4-A* are markers for ectoderm/endoderm and zymogen gland cells respectively (Siebert et al., 2019). We referred to Clusters 0-2 in this analysis as "head epithelial/gland cells", denoting KS1-high and Dkk-high (Figure S3). Cells in clusters 3 and 4 were mostly derived from the 12-hour regeneration time point. The top markers for these clusters had functions associated with reverse transcriptase and mobile elements so we called these cell clusters Transposable Element high or "TE high" (Figure S3; Figure S4). We differentiated cluster 3 from 4 as being "Wnt signaling +" because cluster 3 had cells expressing genes associated with Wnt signaling.

The top markers for Clusters 5 and 6 included genes for zinc finger proteins, a neuroblast differentiation-associated protein *AHNAK*, and a *DEK* isoform (Figure S4). Both clusters had high expression of stem cell and differentiation genes such as *Fos*, *NK2*, *Pax-like*, *SoxC*, *Wnt9/10c*, *piwi* and *vasa (*Figure S4). Cluster 5 markers were predominantly expressed in germline, nematoblast, and interstitial stem cells in the *Hydra* cell atlas, so we called this cluster "interstitial progenitor" cells (Figure S3). Cluster 6 top markers were expressed in epithelial cells, due to expression of stem cell and progenitor differentiation markers, we called this cluster "epithelial progenitor-like". The spatial expression of *Wnt3* and Wnt signaling component genes revealed an overlap in Cluster 6 (Figure S3; Figure S5). To further investigate the potential identity of these cells, we performed subclustering of Cluster 6 cells. These cells separated into 3 subclusters: 6.0, 6.1, and 6.2 (Figure S3), with Wnt signaling genes highly expressed in subcluster 6.2 (Figure S3). The top markers for cluster 7 included genes related to arrestin, fibrilin, calretinin, calmodulin, GTPase, calcium binding and lebircilin (Figure S5), which were more highly expressed in battery and nematocyte cells in the *Hydra* cell atlas, and therefore we called this group "cnidocyte cells". Lastly, the top markers for cluster 8 included neuropeptides *KVamide*, *Hym355* and *LWamide* (Figure S4), so we concluded that this cluster was a neuronal cell cluster. This transcript-level analysis helped guide identification of the nine distinct cell types at the gene-level, generated by adding transcripts, presented above.

Expression in candidate head organizer cells

In the transcript-level analysis, we identified a subcluster of cells that express Wnt signaling components and are likely head organizer cells (Figure S3; Figure S5). The top markers for this subcluster included genes specific to *Hydra*, reverse transcription, mobile elements, stress response, and homologs of genes associated with human cancers (Table S2). Looking specifically

at Wnt3-positive cells within this subcluster, we found *Wnt16*, *Otx2*, *HyAlx*, *β-catenin*, *Wnt9/10c HyBra2*, *Dkk1/2/4A*, *Jun* and *Fos* co-expressed with *Wnt3*. In the gene-level analysis, we were able to identify the head organizer cells as a separate cell cluster. The top markers for this cluster were similar to those of sublcuster 6 (Table S2). In this analysis, we obtained similar patterns of expression with *Wnt16*, *Otx2*, *Egr-like*, *Wnt9/10c HyBra2*, *Jun* and *Fos* co-expressed with *Wnt3*. These genes are known to be involved in regeneration and early wound response in other animals (Petersen et al., 2015; Srivastava, 2021).

Candidate Hydra regeneration genes are predominantly expressed in head organizer cells

Previous bulk RNA-seq studies have identified candidate genes involved in *Hydra* head regeneration (Cazet et al., 2021; Murad et al., 2021; Petersen et al., 2015). We looked at the distribution and expression of those genes and animal development genes in our scRNA-seq clusters (Figure 1D). Overall, we found that Wnt signaling genes and TFs associated with regeneration were predominantly expressed in head epithelial, i-cell, and candidate head organizer cells (Figure 1D; Figure S6).

Wnt3 is the most well studied gene involved in *Hydra* head regeneration. Members of the Wnt signaling pathway that increase in expression early as a response to injury and become hypostome specific after 8 hours include *Wnt3*, *Wnt7*, *Wnt9/10c*, *Wntless*, *β-catenin*, *dishevelled* and *Sp5* (Cazet et al., 2021). We hypothesized that these genes would be expressed in similar cells or cell clusters as *Wnt3*. While the expression and UMAP distribution of these genes varied, they were all expressed in the proposed head organizer cell cluster (Figure S2; Figure S6). In addition to *Wnt3*, previous studies have found expression of TFs involved in animal regeneration to be dynamic with respect to spatial and temporal expression in *Hydra*, including *Jun*, *Fos*, *HyBra1*, and *Otx2* (Cazet et al., 2021; Murad et al., 2021; Petersen et al., 2015). In mice, *Jun* and *Fos* are

involved in liver and skeletal muscle regeneration (Kamp et al., 1995; Morello et al., 1990). In axolotl and planaria, *Jun* and *Fos* are some of the earliest genes expressed after injury (Sabin et al., 2019; Wenemoser et al., 2012). In our dataset, both *Jun* and *Fos* had highest percent expression and average expression in the head organizer cell cluster (Figure 1D). Similar to *Jun* and *Fos*, *Brachyury* is also proposed to have a conserved role in animal patterning (Tewari et al., 2019). In *Hydra*, *HyBra1* functions in head formation with expression localized to the hypostome in adults and developing buds (Technau and Bode, 1999). *HyBra1* is mostly in the endoderm while its paralog *HyBra2* is predominantly expressed in the ectoderm (Bielen et al., 2007). In our single cell analysis, while *HyBra1* expression was highest in TE high cells, *HyBra2* was highest in epithelial cells and the head organizer (Figure 1D). For the *Otx* genes, *Otx2-like* had high percent and high average expression in the head organizer while *Otx1-like* was not expressed in this cell cluster (Figure 1D).

In addition to identifying TFs with temporal dynamic expression during *Hydra* head regeneration, studies have also identified dynamic binding of TFs including *Gsc*, *Pax*, *Fox* and *Sox* (Cazet et al., 2021; Murad et al., 2021). We found *Gsc* most highly expressed in the head organizer and i-cells (Figure 1D). For *Pax* genes, we found *PaxA* to be most highly expressed in the nematoblast cells. This was expected since it has a suggested to function in nematogenesis (Siebert et al., 2019). *PaxB* was highest in i-cells and *PaxC* was highest in epithelial and head organizer cells. We identified 19 members of the *Fox* gene family, many of which had higher expression in interstitial progenitor and cnidocyte cell clusters (Figure S7). One of these genes included *FoxO*, a stem cell regulator in *Hydra* (Figure 1D) (Boehm et al., 2012). Finally, for *Sox* genes we identified 12 genes (Figure S8). *SoxC* was previously described as a marker for differentiating types and had localized expression in neuron progenitor and nematoblast cells (Siebert et al.,

2019). Supporting this hypothesis, we find *SoxC* predominantly and highly expressed in i-cells (Figure 1D).

Bulk-RNA gene co-expression modules match distinct cell clusters

We used WGCNA to analyze our previously published bulk RNA-seq data from the hypostome over 7 time points of head regeneration. WGCNA clustered 16,971 genes into 31 modules, which are groups of tightly co-expressed gene sets ranging from 50 to 3420 genes. We found *Wnt3* co-expressed with 1506 other genes in the darkgreen module (Figure 2A, Table S3). The module eigengene for the darkgreen module was significantly correlated in the adult hypostome and decreased in correlation from 12 hrs to late in regeneration at 48 hrs (Figure 2B). In addition to *Wnt3*, this module included other *Wnt* gene family members *Wnt7, Wnt9/10c, Wnt5a*, *Wnt8* and *Wnt9/10a (*Table S3). Other candidate wound response and regeneration genes that were co-expressed with *Wnt3* in the same module included*, HyBra1, Dishevelled, Meis1-like, COUP-TF, HyAlx, PaxC, Pax6, Sox2-like*, *Sox18-like, Sox14-like* and *β-catenin-like* (Table S3). The *Wnt3* antagonist *Sp5* was also found in the same module as *Wnt3*. GO analysis of the darkgreen module revealed that the *Wnt3* co-expression network was primarily involved in transcription and translation processes, cellular signaling, cell differentiation and metabolic processes (Figure S9). GO terms associated with rRNA processing, cell division, cell commitment, cell signaling, and negative regulation of transcription were the most significantly enriched biological processes in the *Wnt3* co-expression network (Figure 2C).

Since *Jun* and *Fos* are early wound response genes co-expressed with *Wnt3* at the single cell level and have some of the highest percent expression in the head organizer cells, we looked for them in our co-expression modules. While not in the darkgreen module, *Jun* and *Fos* are both found in the same co-expression network and co-expressed with 444 genes (coral2 module; Table

S4). The module eigengene for the coral2 module starts to be positively correlated at the 4 hrs post bisection timepoint and increases in correlation with the strongest correlation at the 12 hrs timepoint. (Figure 2B). The coral module is primarily involved in innate immunity, cell growth, and differentiation (Figure 2D; Figure S9). GO terms associated with regulation of cell growth, cell migration, cell proliferation, and epidermal and fibroblast growth factor receptor signaling were some of the most significantly enriched processes associated with the *Jun/Fos* co-expression network (Figure S2; Figure S9). The coral2 module has the largest and significant gene overlap with head organizer, nematoblast/cnidocyte, and interstitial stem cells.

The *Wnt3* co-expression module has the largest number of genes overlapping with the head organizer and i-cells clusters (Figure 3A). It has a significant correlation to endoderm and ectoderm which is not surprising as *Wnt3* is a marker for hypostome epithelial cells (Lengfeld et al., 2009; Siebert et al., 2019). The genes that overlap between the darkgreen module and Wnt3+ cells include genes that function in Wnt3 signaling (*Daple*), proto-oncogenes (*Ret*), transcription factors, growth factors, mobile elements, and reverse transcriptase (Figure 3B).

Gene expression in pseudotime

We extracted clusters 0,1,5, and 6 that had more than three *Wnt3*-positive cells to identify candidate genes upstream, downstream, or co-expressed with *Wnt3* using pseudotime analysis. Cells were separated into 5 states with 2 branch points (Figure 4A). Pseudotime zero and state 1 were mostly made up of interstitial progenitor cells, state 2 branch terminated with interstitial progenitor cells, state 4 terminated with candidate head organizer cells, and state 5 was predominantly made up of head epithelial cells. The *Wnt3* positive cells states were State 1 and State 4. Candidate regeneration genes with similar expression trajectories to *Wnt3* in this analysis included Wnt signaling genes (Figure 4; Figure S10). Some of the genes that were expressed

immediately before *Wnt3* and may be correlated with *Wnt3* expression included *Nkx2*, *Wnt5a*, *Dkk1/2/4A*, *SoxC*, *Sox17* and *Sox18 (*Figure 4B; Figure S10; see Discussion). At the gene-level, the clusters that had more than 3 *Wnt3*+ cells were the head organizer and epithelial cells. In pseudotime, these were arranged into 5 stages, 2 of which had *Wnt3* signaling expression (Figure S10). One of the states proceeded from injury to t4 early regeneration and the other terminated in the hypostome steady state organizer (Figure S10). *Wnt3* had similar trajectories to *Wnt16*, *Sp5*, *Dishevelled*, *Frizzled2*, *Frizzled4*, *Sox2-like*, and *PaxC* (Figure S10).

Wnt3 cis-regulation

To identify which, if any, of these pseudotime-correlated genes may be directly regulating *Wnt3*, we searched its candidate *cis*-regulatory regions for footprint signatures of bound transcription factors. Previous studies using ATAC-seq and ChIP-seq identified peaks at the *Hydra* promoter and one upstream putative-enhancer region (Cazet et al., 2021; Murad et al., 2021; Nakamura et al., 2011b). Using combined hypostome ATAC-seq data (Murad et al., 2021; Siebert et al., 2019), we found potential binding motifs at the enhancer region for homeodomain, basic leucine zipper (bZIP), and DM-type intertwined zinc finger TFs (Table S5). TFs included members of the Fork head, STAT, and Nk families, such as Nkx2 (Table S5). We found binding motifs in the promoter for homeodomain, C2H2 zinc finger, basic helix-loop-helix (bHLH), and High-mobility group (HMG) domain factors that match TFs such as including Sox11 and Six3/6 (or Optix) (Table S5). Using only hypostome data that we previously generated (Murad et al., 2021), we found transcription factor binding motifs in the Wnt3 promoter for the Sox family (Sox2, Sox11, Sox13, Sox17, Sox18), and Six3/6 (Table S5).

Discussion

The cellular organization and actions of the *Hydra* head organizer are topics of high interest in comparative developmental biology. While there have been fundamental studies investigating candidate genes using *in situ* hybridization and chemical inhibition, we can now expand on these findings using single cell transcriptomics to identify additional genes and pathways that allow for head regeneration. In this study we have generated a cell atlas and cell trajectories for *Hydra* head regeneration. We were able to identify 9 cell types in the regenerating tissues, including candidate head organizer cells. In addition, by generating cell trajectories for regenerating tissues we identified potential regulators of Wnt/β-catenin signaling including members of the Six and Sox gene families. By re-analyzing bulk RNA-seq and ATAC-seq data, we find that co-expression and binding patterns that are confirmed by our single cell data, further supporting our findings.

A role for transposable elements during Hydra head regeneration

Approximately 50% of the *Hydra* genome is made up of transposable elements (Chapman et al., 2010). The organismal function of transposable elements (TEs) remains largely unknown with some hypothesizing that they function in gene regulation (Bourque, 2009; Slotkin and Martienssen, 2007). In mammals, TEs are highly expressed in embryos during zygotic genome activation and in pleuripotent cells at different stages (Gerdes et al., 2016; Hackett et al., 2017; Low et al., 2021). Whether TE expression is due to global opening of the chromatin or whether TEs play an essential role in regulating shifts in expression is still being investigated (Gerdes et al., 2016; Low et al., 2021). TEs have been shown to affect chromatin accessibility and even to have post-transcriptional effects thus it is hypothesized that they have a role in pleuripotency (Hackett et al., 2017). In terms of regeneration, increase in TEs were detected in regenerating haematopoietic stem cells and overexpression of TEs led to their activation (Clapes et al., 2021). In the sea cucumber *Holothuria glaberrima*, it was found that changes in transcription

of retrotransposons were associated with tissue regeneration (Mashanov et al., 2012). In *Hydra*, retrotransposons increase in expression from 0 to 12 hours during head regeneration (Petersen et al., 2015). In this study, we found expression of several genes related to reverse transcription and transposable elements. Some of these genes were top markers and most abundant and highly expressed in the cells we labeled "TE high". Our findings suggest a role for transposable elements in *Hydra* head regeneration particularly at 12 hours. This increased expression of transposable elements is reminiscent of a stark shift in gene expression at 12 hours for genes differentially expressed between regeneration and budding (Murad et al., 2021). In this study, TEs are co-expressed with *Wnt3* in the darkgreen module and with *Jun/Fos* in the coral2 module respectively (Table S3-4). Following similar patterns of TE expression as our single cell analysis, we found a change in correlation of the expression for the darkgreen module from 12 hours to 48 hrs and the strong correlation for the expression of coral2 module at 12 hrs (Figure 2). Moreover, some of these mobile elements are co-expressed with *Wnt3* at the single cell level (Figure 3). Thus, it is likely that transposable elements play a role in regulating the transcriptomic shift important for hypostome regeneration at around 12 hours post-bisection in *Hydra*.

Injury and early regeneration in Hydra

Using WGCNA on bulk RNA-seq, we found two modules of interest: coral2 consisting of genes co-expressed with *Jun*/*Fos* and darkgreen with genes co-expressed with *Wnt3*. The coral2 module begins expression at 4 hours and peaks at 12 hours and Jun/Fos are considered early response factors that potentially have conserved roles early in regeneration (Srivastava, 2021). This module increases early during the wound healing phase and is enriched for functions in cell growth and migration, epidermal growth factor response (EGFR) signaling, and immunity (Figure 2; Figure S9). While the functions of EGFR in regenerating *Hydra* has not been established, in

Drosphila, EGFR and MAPK act downstream of JNK (Jun N-terminal kinase) signaling (of which *Jun* and *Fos* are key components) during apoptosis-induced proliferation (Fan et al., 2014). Other genes associated with this module included Toll (TLR) and tumor necrosis factor (TNFR) receptors (Table S4). This is consistent with a proposed immune response to injury in *Hydra* associated with early expression of *Jun*, *Fos*, TLR and TNFR signaling genes (Wenger et al., 2014).

Unlike coral2, genes in the darkgreen module turn on later during regeneration (Figure 2). Wnt signaling is highly conserved in evolution and is known to play a role in cell proliferation, cell fate determination, cell migration during development and regeneration. As expected, the co-expression module containing *Wnt3* is primarily involved in cell division, cell fate commitment and differentiation most likely directing cell differentiation and growth during regeneration. Genes controlling cell cycle and cell death are known to be expressed during regeneration and are enriched in this co-expression module, such as cyclin-dependent kinases (CDKs), receptor type protein tyrosine phosphatases (RPTPs), and ATM serine kinases (Petersen et al., 2015). While the coral2 genes are responding to injury and involved in wound healing, the genes in the darkgreen module are active in regeneration or *de novo* tissue development.

scRNA-seq clarifies bulk RNA-seq results by confirming cell-level co-expression

WGCNA on bulk RNA-seq allowed us to compare results from a previous time course in regeneration to our single cell data. Genes found to be co-expressed with *Wnt3* in the darkgreen module that also had similar expression trajectories in pseudotime included genes associated with Wnt signaling such as *Wnt7*, *Wnt9/10a*, *Wnt9/10c*, *Dishevelled*, and *Sp5*. *Wnt7*, *Wnt9/10a*, and *Wnt9/10c* were previously found to be expressed by *in situ* hybridization in the adult hypostome, during budding, and during regeneration with similar patterns to *Wnt3* thus their coordinated

expression is not surprising (Lengfeld et al., 2009). In addition, *Wnt7*, *Wnt9/10c*, *Dishevelled*, and *Sp5* are turned on and have similar expression trajectories in *Hydra* head and foot regeneration (Cazet et al., 2021). The similarity in expression dynamics of *Wnt3* and *Wnt3* signaling genes across multiple independent studies highlight their role in *Hydra* head regeneration (Figure 5).

Other genes that overlapped in these two analyses included *Wnt5b*, *HyAlx, PaxC*, *myb-D*, *myb-X, Sox2-like, Sox18. Wnt5a* and *HyAlx* are markers of the *Hydra* tentacles (Philipp et al., 2009; Smith et al., 2000), it is possible that their increase in expression during hypostome regeneration is associated with early tentacle formation rather than with head organization because neither of these genes is expressed in the head organizer cell cluster (Figure 1D). On the other hand, it has been suggested that, in *Hydra*, *Wnt5a* is regulated by TCF/β-catenin (Philipp et al., 2009). This is supported by enrichment of enhancers at this gene when canonical Wnt is activated (Reddy et al., 2020). These findings taken together with the co-expression of *Wnt5a* and *Wnt3* in WGCNA suggest that *Wnt5a* may synregize with *Wnt3* and may play a complimentary role during head regeneration.

In cnidarians, *PaxA* functions in cnidocyte development but the role of *PaxC* has not yet been determined (Babonis and Martindale, 2017; Siebert et al., 2019). In our study, we find *PaxC* expression in head organizer cells, *PaxC* expression follows a similar trajectory to *Wnt3*, and *PaxC* is co-expressed with *Wnt3* in the WGCNA analysis. Taken together, these results suggest *PaxC* has a role in patterning during head regeneration. Supporting this is the enrichment of Pax5 and Pax6 binding motifs for dynamic accessibility during *Hydra* head regeneration (Murad et al., 2021). These binding motifs are annotated for known vertebrate motifs, so the *Hydra* binding factor remains to be confirmed. Like *PaxC*, *myb-D* and *myb-X* are found in the *Wnt3* module and have similar cell trajectories in pseudotime, but these genes are also tightly co-regulated with *Wnt3*

and are co-expressed at the single cell level (Figure 3B). The functions of these genes in *Hydra* are currently unknown but our results reveal a role in the *Hydra* head organizer.

Potential Wnt3 regulators

Pseudotime analysis allowed us to identify genes that may be interacting with and regulating *Wnt3*. *Nkx2*, *Wnt5a*, *Dkk1/2/4A*, *SoxC*, *Sox17*, and *Sox18* were expressed immediately before *Wnt3* expression increases. *Nkx* is associated with foot formation (Siebert et al., 2005). An *Nkx2-like* gene has also been found to be differentially expressed during *Nematostella* regeneration and a homolog has been suggested to be a downstream target of Wnt signaling in *Hydra* (Reddy et al., 2019; Schaffer et al., 2016). In our study an *Nkx2* was expressed before *Wnt3* and had high expression in late State 5 cells together with *HyBra1*, *β-catenin*, *Frizzled-4*, *Jun* and *Fos*, which are all targets of *Wnt3 (*Figure 5). Moreover, in our ATAC-seq analysis we found an *Nkx2* binding motif at the *Wnt3* enhancer region. We propose that *Nkx2* is a possible regulator of *Wnt3*. While *Dkk1/2/4C* does not appear to be binding the *Wnt3* promoter or enhancer, it acts as a canonical Wnt/β-catenin antagonist. Yet, a member of this gene family is expressed early during hypostome regeneration (Guder et al., 2006). *Dkk1/2/4A* and *Wnt3* are co-expressed at the single cell level within the head organizer cell cluster. Interestingly, *Wnt5a* and *Dkk1/2/4A* interact to function as TCF/β-catenin activators in mammalian tissue repair (Guder et al., 2006; Miyoshi et al., 2012). We predict that in a regenerating *Hydra* head *Dkk1/2/4A* may enhance canonical Wnt signaling in *Hydra* (Figure 5). Lastly, we found in our pseudotime analysis that *Sp5* has contrary expression to *Wnt3*. This is expected, as *Sp5* is a Wnt antagonist (Vogg et al., 2019). Sp5 acts as a *Wnt3* repressor and its knockdown results in a *Hydra* polyp with multiple heads (Vogg et al., 2019). We predict that after bisection *Wnt3* is turned on as a response to injury, *Sp5* is then turned on by TCF/β-

catenin so that not all cells produce new heads, then *Wnt3* returns to normal expression in the intact head as an organizer (Figure S10).

A conserved role for Sox and Six3/6?

SoxC, *Sox17*, and *Sox18* had pseudotime expression before *Wnt3* and *Sox2-like* had an expression trajectory similar to *Wnt3*. In *Hydra*, *SoxC* is expressed in progenitor cells that are undergoing differentiation into neurons and nematocytes (Siebert et al., 2019). We found *SoxC* was more highly expressed in i-cells as would be expected and likely does not have a direct role in head organization but is important for the development of neurons in the regenerating head (Figure 1). *Sox2-like*, *Sox13* and *Sox18*, on the other hand, were expressed in the head organizer cell cluster (Figure S8). Moreover, *Sox2-like* and *Sox18* were co-expressed with *Wnt3* in the WGCNA analysis. Interestingly, Sox2, Sox11, Sox13, Sox17, and Sox18 are candidate bound TFs at the *Wnt3* promoter (Table S5). Multiple Sox genes have been shown to have regulatory functions for Wnt signaling. As an example, Sox2 interacts with Wnt signaling and is important for neuron regeneration in sea star larvae (Kormish et al., 2010; Zheng et al., 2022). Sox13 is a TCF repressor and is proposed to control Wnt signaling in embryo development (Marfil et al., 2010). *Sox17* was not expressed in the head organizer, but it was expressed in progenitor and epithelial cells which could physically be near the head organizer. In *Xenopus*, XSox17α, XSox17β, and XSox3 bind β-catenin to inhibit Wnt signaling during embryo development (Zorn et al., 1999). Finally, recent work suggests a link between *Sox18* and Wnt signaling in cancer (Geng et al., 2020; Kormish et al., 2010; Yin et al., 2017).

As Sox has been shown to directly modulate Wnt signaling in vertebrates, we predict that one or more of the *Sox* genes play a role in *Wnt3* signaling in *Hydra* (Figure 5). One question of interest is whether the functions of Sox as a Wnt regulator are conserved or if these actions have

been co-opted in animal evolution. In the examples above Sox genes repress Wnt by two different mechanisms, binding β-catenin or TCF. Our data suggests candidate Sox are acting directly as Wnt agonists in *Hydra* regeneration by binding a *cis*-regulatory site. These comparisons suggest co-option of different Sox family members at different points in the signaling cascade, but a constraint on the evolution of this gene regulatory network (Kopp, 2009).

Optix is a member of the sine oculis homeobox (SIX) gene family. *Six3/6* functions in patterning in *Nematostella* (Sinigaglia et al., 2013). Members of the *Six* gene family have been found to have roles in eye regeneration in jellyfish and newts (Grogg et al., 2005; Stierwald et al., 2004). In our analyses, we found a bound TFBS for Optix (Six3/6) at the *Wnt3* promoter and expression of *Six3/6* in the *Hydra* head organizer cell cluster. These results together indicate that *Six3/6* could also be a *Wnt* regulator. In mice, Six3 and Six6 repress Wnt signaling (Diacou et al., 2018). It could be that members of the *Sox* and *Six* gene family have a role in Wnt signaling across species. In this case it is the homologous *Six3/6* in multiple species, but the direct regulation of Six TFs on *Wnt* or their mechanisms of interaction have not been functionally described. The question of whether regeneration is homologous or due to homoplasy is currently being debated in the literature (Srivastava, 2021). Our findings and previous work do not yet determine whether regenerating animals are using homologous genes from one origin or whether similar developmental genes are constantly being co-opted for regeneration.

Comparing regeneration in Hydra to Hofstenia, Planaria, and Nematostella

In order to understand the degree to which regeneration is conserved or divergent across species, we need to compare the underlying genes and regulatory programs in regenerating species of different taxa. A comparison of genes involved in head and tail regeneration between planaria and *Nematostella* is summarized by Schaffer et al. 2016 (Schaffer et al., 2016). This study found

orthologous genes expressed in anticipated patterns (based on the organisms oral and aboral development) for axial regeneration such as *Otx* and *Six* (Schaffer et al., 2016). We find both of these genes associated with head regeneration in *Hydra*. Genes that were associated with head regeneration in both *Nematostella* and planaria included *SoxB*, *Wnt2*, and *FoxD* (Schaffer et al., 2016). In *Hydra*, members of these gene families were expressed in epithelial and progenitor cells, but we are unable to state whether these are paralogs or orthologs that have a conserved function in head regeneration. Genes that are associated with regeneration in *Nematostella* head and planaria tail include *Wnt1*, *Wnt4*, *Wntless*, *Wnt11*, and *Wnt16* (Schaffer et al., 2016). A similar pattern arises when we look at Wnt genes in *Hydra* and the acoel *Hofstenia*. In *Hofstenia*, *Wnt3* and other genes associated with *Hydra* head regeneration were found to function in posterior regeneration. These genes included *Brachyury*, *Sp5* and *FoxA1* (Ramirez et al., 2020). Moreover, Egr is the proposed regeneration initiation factor in *Hofstenia.* In a comparison of chromatin accessibility during regeneration between *Hostenia* and a planaria Egr was one of the most accessible motifs along with Fox and Jun/Fos. We found *Egr-like*, *Jun*, and *Fos* expressed in head organizer cells and co-expressed with *Wnt3*. This comparison across species highlights the roles of Wnt signaling and TF activity of Egr, Wnt, Fox, Jun, Fos, Sox, Otx and Six in regeneration and patterning.

Overall results from our study and previous studies highlight that some of the same gene families important to development are used by animals for regeneration. However, the expression trajectories and genetic programs underlying patterning vary between normal development and regeneration. Moreover, while the same gene families might be used, the gene family members used and their expression in oral versus aboral regeneration can vary across organisms. Instances where gene network connections appear conserved, such as the role of Sox and Six in *Wnt*

signaling regulation, is where future work should focus. Similarly, TEs seem to play a role in regeneration competency and pluripotency in different taxa. While the direct role of TEs is yet unknown, here we find that an increase in TE expression is correlated with shifts in gene expression suggesting a direct role in gene regulation. Investigating how development and regeneration are similar across animals, can lead to insights about how development goes awry and why some organisms are more capable of regenerating certain cell types and tissues. Through this research we can learn more about how to disrupt or fix these essential pathways that lead to disease.

Method details

Animal care

Hydra vulgaris (strain 105) were maintained in glass pans in the laboratory at room temperature in *Hydra* medium (4.22 g calcium chloride dehydrate, 3.06 g magnesium sulfate anhydrous, 4.2 g sodium bicarbonate, 1.1 g potassium carbonate in 100 liters of DI water). *Hydra* were fed brine shrimp (*Artemia salina*) twice per week and cleaned after every feeding. To clean the containers, *Hydra* medium with brine shrimp was poured out and any detached *H. vulgaris* were recovered. New *Hydra* medium was added so that fed *H. vulgaris* were left submerged in about 2 inches of medium. *H. vulgaris* were starved 1-3 days prior to RNA extractions to avoid brine shrimp contaminations.

Regeneration time course and cell dissociation

12-15 *H. vulgaris* individuals were used for each sample time point for a total of 3 timepoints (t0, t4 and t12) and the hypostome (Figure 1B). For the hypostome sample, the head was bisected, the tentacles were removed and the hypostome was collected (Figure 1B). For t0, the hypostome was bisected and the tissue directly below it was immediately collected (Figure

1B). For timepoints t4 and t12, the hypostome was bisected then *Hydra* were left in medium at room temperature to heal and regenerate for 4 and 12 hours, respectively. For each time point, the regenerated tissue was collected (Figure 1B). The collected tissues were pooled in a 1.5 ml tube for each sample and washed with *Hydra* medium. The medium was then removed and *H. vulagris* were dissociated using Pronase E as previously described (Greber et al., 1992). Briefly, 1 ml of *Hydra* dissociation medium with ~75u/mL Pronase E (VWR, Radnor, PA) was added to each sample. Samples were placed on a nutator for 90 minutes. Cells were washed through a 70µm cell strainer (Corning, Corning, NY) then centrifuged at 300xg for 5 minutes at room temperature. Pellets were resuspended and strained through a 40µm cell strainer (Corning, Corning, NY). The final sample was resuspended with 60 µl 1X PBS containing 0.01% BSA. Cells were counted on a TC20 Automated Cell Counter (Bio-Rad, Hercules, CA).

scRNA sequencing

Immediately after dissociation, cells were diluted to 2500 cells/µl in 1X PBS containing 0.1% BSA. 4.5 µl of sample were used to generate single cell RNA-Seq libraries by following the Illumina Bio-Rad SureCell WTA 3' Library Prep Guide (Illumina, San Diego CA and Bio-Rad, Hercules, CA) and using the ddSEQ Isolator for Single Cell Sequencing (Bio-Rad, Hercules, California). Libraries were quantified and quality checked using a bioanalyzer (Agilent, Santa Clara, CA). Libraries were then multiplexed and sequenced using the setting “paired end, R1:68 cycles, R2:75 cycles” on a NextSeq 500 sequencer (Illumina, San Diego, CA).

Quantification and Statistical analyses

scRNA-seq clustering and pseudotime

Individual cells were identified from demultiplexed libraries using ddSeeker v.1.2.0 (Romagnoli et al., 2018). A transcriptome from Murad et al. (Murad et al., 2021) was indexed and

mapped using kallisto v. 0.46.1 (Bray et al., 2016). Abundances were grouped into a gene matrix for each sample using a custom script, which we refer to as the transcript-level analysis. Counts data were loaded into R and analyzed using Seurat v. 4.0.0 (Butler et al., 2018; Stuart et al., 2019). Briefly, Seurat objects for each sample were made using min.cells = 1, min.features = 120. Each object was then assigned a time during regeneration (t0, t2, t4, t12, hypo). The 5 individual objects were then merged into one large Seurat object, log normalized using scale.factor = 10000. We identified variable features using selection.method = "vst", nfeatures = 2000. After finding neighbors, clusters, and running UMAP, we identified the top markers of each cluster. We also looked for our known candidate genes and their expression. The transcript-level analysis was for additional resolution as previously done for Hydra to capture reads on transcripts not represented in the hydra gene models (Siebert et al., 2019). The transcript-level analysis helped guide the gene-level cell identification. In addition, we also performed a gene-level analysis by adding transcripts matching the same gene ID in the count analysis and repeating the analysis as described above.

For pseudotime analysis, we extracted gene expression information for all clusters with at least 3 Wnt3+ cells. The expression data were input into Monocle v. 2.18.0 (Qiu et al., 2017) where we did an unsupervised clustering and unsupervised trajectory correcting for batch effects. We visualized results by generating heatmaps for the top 50 or 100 genes that differentiate cell type and significant (qval <0.01) genes of interest (our candidate regeneration genes). Candidate genes were visualized for expression in pseudotime along branches of interest.

Identification of Wnt3 Transcription Factor Binding

Raw read ATAC-seq data for the *Hydra* hypostome (2 replicates) were obtained from GEO GSE127277 (Murad et al., 2021). Reads were trimmed using Trimmomatic v. 0.39 (Bolger et al., 2014) then mapped to the genome using bwa v. 0.7.17 (Li and Durbin, 2009). Homer v.

4.11.1 was used to call peaks. Peaks and bam files for the two biological replicates were then merged before performing downstream analysis with TOBIAS v. 0.12.10 (Bentsen et al., 2020). We used ATACorrect, FindPeaks and BINDetect to identify peaks and bound TFBS. For a combined analysis, to improve resolution and recover enhancer peaks, additional hypostome ATAC-seq data (3 replicates) were obtained from GEO GSE121617 (Siebert et al., 2019). Data for the 5 replicates were processed similar to above and in Seibert et al (Siebert et al., 2019). After trimming, reads were mapped to the *Hydra* mitochondrial DNA and genome using bowtie2 v. 2.4.1 (Langmead and Salzberg, 2012). Mitochondrial reads were removed using Picard v. 2.26.3. Peaks were called using Homer v. 4.11.1 and binding calculated using TOBIAS v. 0.12.10.

WGCNA analysis on Bulk RNA-seq

Bulk RNA-seq data of the *Hydra* hypostome tissue and head regeneration time points (0, 2, 4, 6, 12, 24, and 48 hours) were obtained from GEO accession GSE127279 (Murad et al., 2021). The dataset consists of a total of 16 samples, with 2 biological replicates for both the hypostome tissue and for each head regeneration time point. Raw reads were mapped to the reference transcriptome (Murad et al., 2021) using Kallisto (Bray et al., 2016).

Weighted gene co-expression analysis was performed using the WGCNA package v. 1.70-3 in R (Langfelder and Horvath, 2008). Genes with counts less than 10 in more than 2 samples were removed to reduce noisy, non-significant correlations. After filtration of lowly expressed genes, the input expression matrix consisted of 16,971 genes. Expression of these genes was normalized with the variance-stabilizing transformation function of DESeq2 v. 1.28.1 (Love et al., 2014). To achieve a network with scale-free topology, a soft threshold of 18 was selected using the "pickSoftThreshold" in WGCNA package and the adjacency matrix was created with a

"signed" network. Modules, or groups of genes that are highly co-expressed across samples were generated using a hierarchical clustering algorithm. A threshold of 0.2 and minimum module size of =30 were used to merge similar expression profiles to obtain 31 modules. The *Wnt3* co-expression network has over 1000 genes and because visualization of all the genes and their interactions would be difficult to illustrate, we only selected genes the top 38 annotated genes that have strong connectivity with *Wnt3*.

The *Hydra* transcriptome was annotated using Blast2GO (Conesa et al., 2005). GO terms enrichment analysis for candidate modules was carried out using TopGO v. 2.41.0 (Alexa and Rahnenfuhrer). GO enrichments of the module containing *Wnt3* and all the co-expressed genes were used as the test dataset and the GO enrichments of all the annotated genes from the transcriptome were used as the universal dataset. To determine overlap between the *Wnt3* co-expression network generated from the RNA-seq data of the hypostome tissue and head regeneration timepoints and Seurat clusters, we performed a Fisher exact test to determine the significance of the overlap.

Data and code availability

Raw single cell RNA-seq data and counts matrices with counts generated and analyzed for this paper are available under GEO accession GSE193277. R and shell scripts accompanying this paper were deposited in zenodo DOI:10.5281/zenodo.5823398. All scripts and data tables for WGCNA analyses are in GitHub https://github.com/lmesrop/WGCNA-bulk-RNAseq-and-single-cell-RNAseq-Hydra-Project.

Acknowledgements: We thank Rob Steele for Hv105 animals, advice on rearing *Hydra*, and feedback on this manuscript; Stefan Siebert for advice on *Hydra* single cell dissociation; Klebea

Carvalho, Gabriela Balderrama-Gutierrez, Katherine Williams, and Camden Jansen for advice on processing and analyzing single cell data.

Author Contributions: AMM and AM designed the study. AMM and HL conducted experiments. AMM analyzed single cell RNA-seq and bulk ATAC-seq. LYM analyzed bulk RNA-seq. AMM wrote the manuscript with consultation from all authors.

Declaration of interests: The authors declare no competing interests.

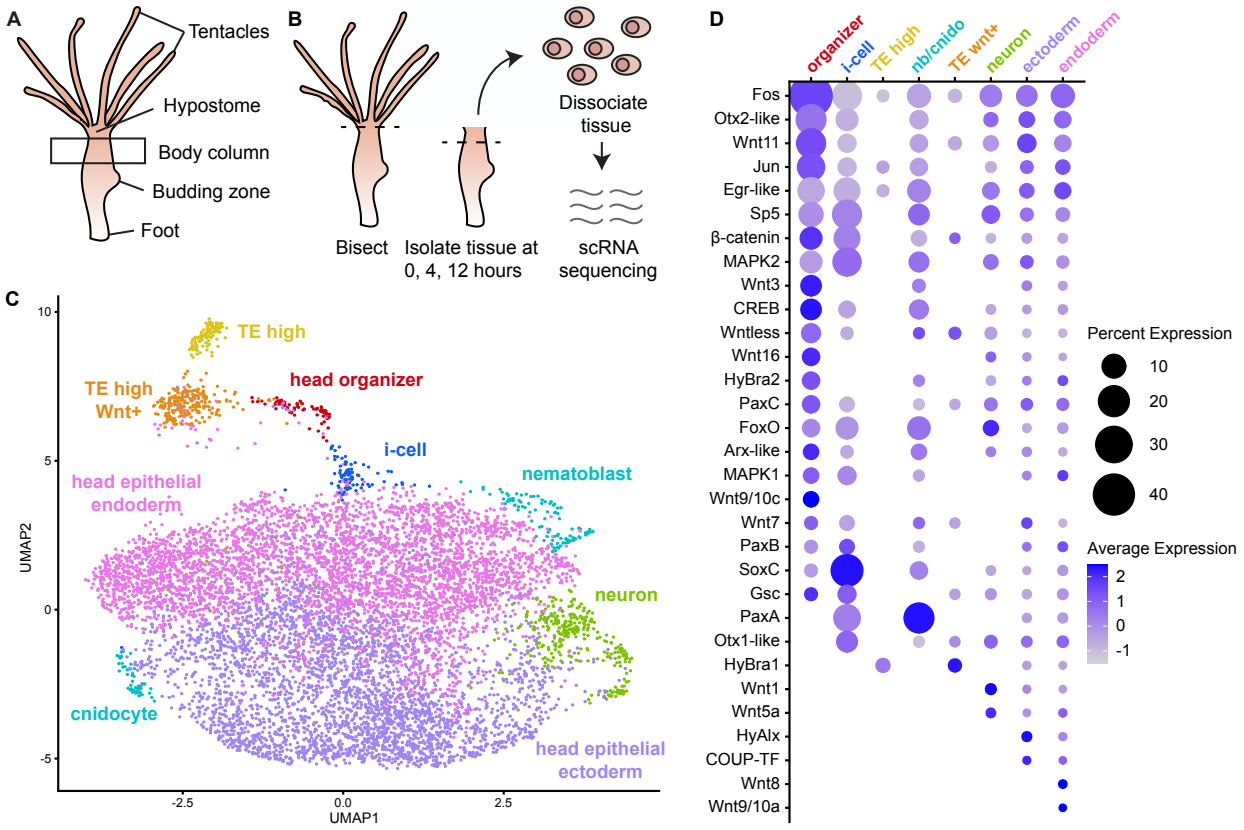

Figure 1. The regenerating *Hydra* hypostome is composed of nine cell types. A) The *Hydra* body plan consists of tentacles, hypostome, body column, budding zone, and foot. B) For a regeneration time course, *Hydra* were bisected below the hypostome, and the adjacent tissue was collected at 0 hr, 4 hr, and 12 hrs. The dissected tissues were dissociated into single cells, mRNA was extracted and sequenced. C) UMAP of cell clusters annotated with cell types. We identified nine distinct cell types in the regenerating head. D) Dotplot showing average and percent expression of candidate regeneration and developmental genes in the different cell types.

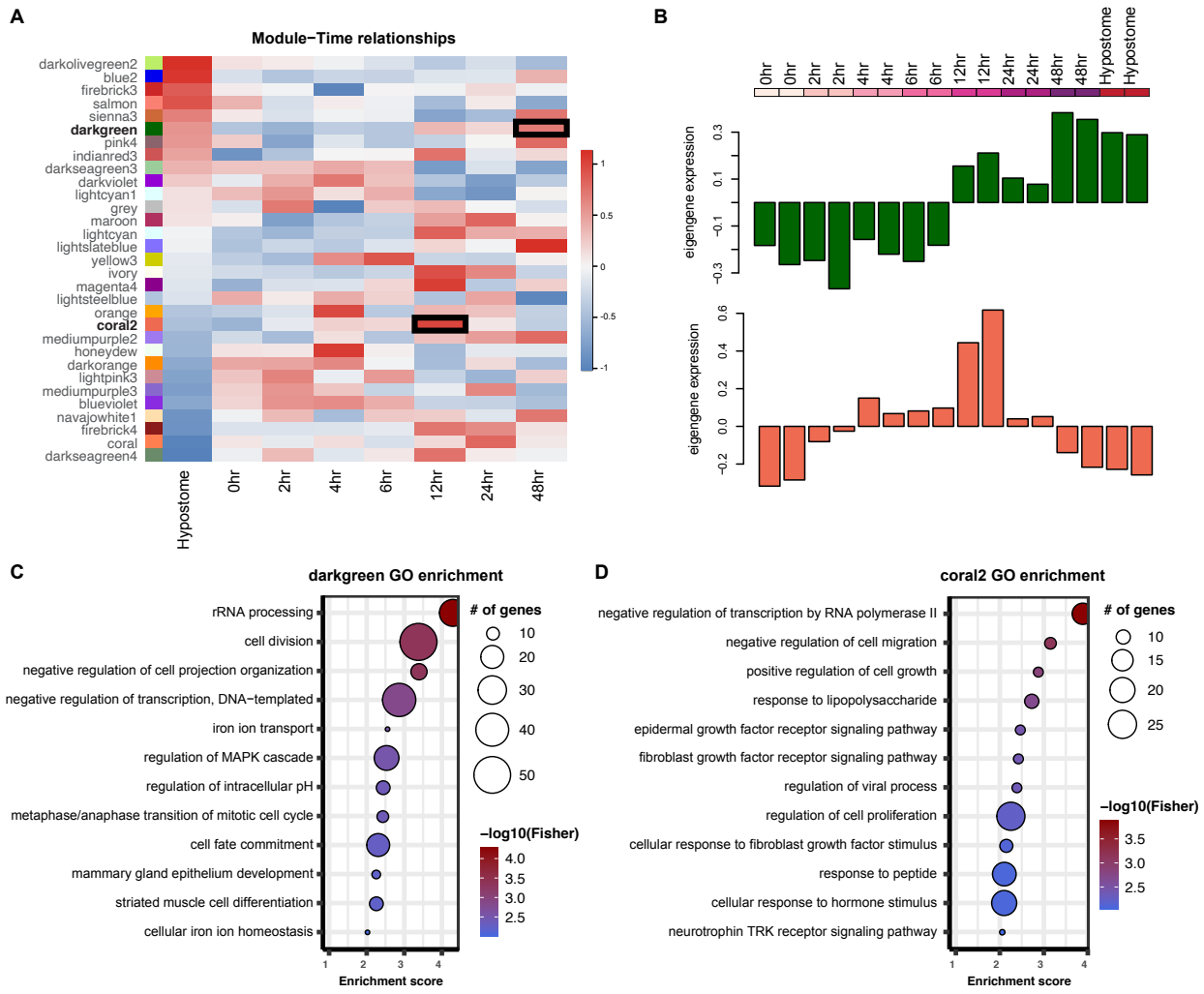

Figure 2. WGCNA reveals co-expression networks related to regeneration. A) Heatmap showing the correlations of module eigengenes to hypostome tissue and regeneration timepoints. *Wnt3* is found in the darkgreen module and Jun and *Fos* in the coral2 module. Boxes indicate significant correlations for our two modules of interest. B) Eigengene expression for the darkgreen and coral2 modules during head regeneration. C) Gene Ontology (GO) enrichment for the darkgreen module > 5 genes. Size of circle indicates number of genes in the GO term category and color is the statistically significant p-value score in logarithmic scale. D. GO enrichment for the coral2 module.

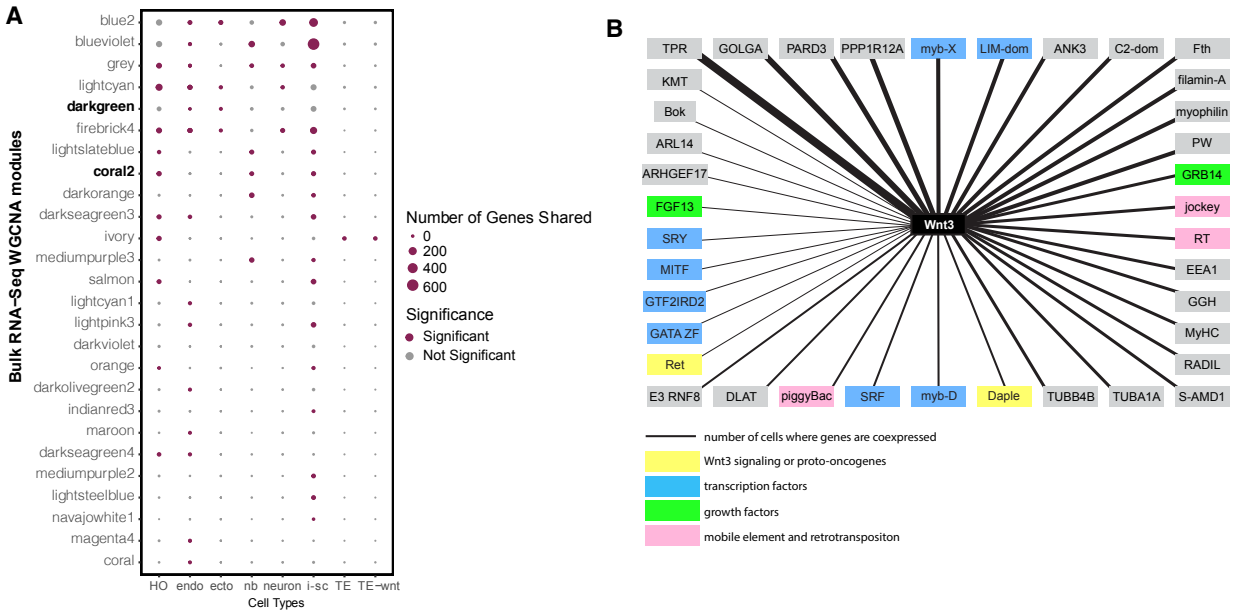

Figure 3. The Wnt3 co-expression module has correlated with the head organizer and i-cells.

A) Correlation of modules to cell types in the Seurat analysis. Size of the circle is number of genes and color depicts a significant correlation with a p-value < 0.05. Only modules with significant correlations are shown. HO, head organizer; endo, endoderm; ecto, ectoderm; nb, nematoblast; neuron; i-sc, interstitial stem cell; TE transposable element high; TE-wnt transposable element high with Wnt signaling. B) Top 38 annotated genes in the darkgreen module co-expressed with *Wn3* at the single cell level. Weight of connection represents number of cells in which the genes are co-expressed ranging from 1-8 cells. *Wnt3* is shown in black, genes that function in *Wnt3* signaling and proto-oncogenes are in yellow, transcription factors are in blue, growth factors are in green, mobile elements and reverse transcriptase in pink, and all other genes are in gray.

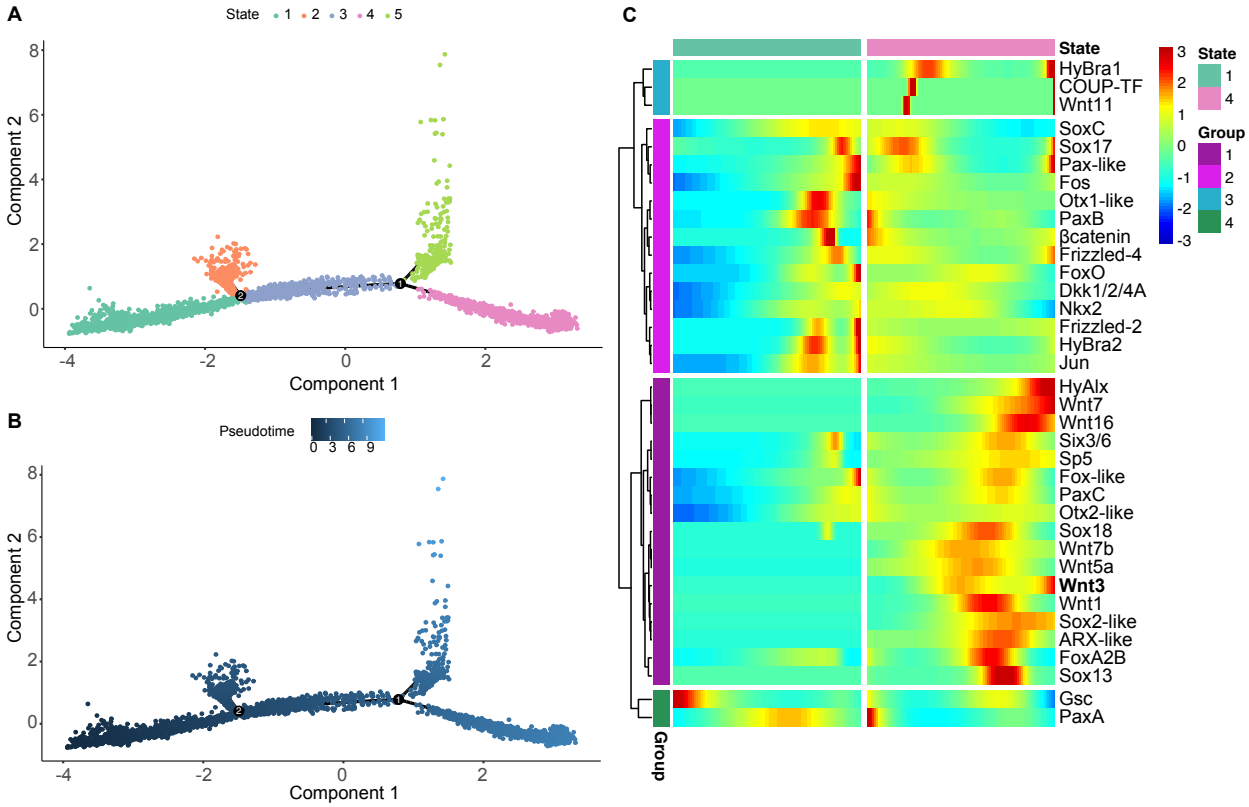

Figure 4. Pseudotime trajectory for *Wnt3*-positive cell clusters reveals potential Wnt3 regulators. A) Cell trajectory for cells from Seurat clusters that had more than 3 *Wnt3*-positive cells. Cells divide into five states with two branch points. B) Pseudotime for the five cell states. C) Expression of significant candidate genes plotted for *Wnt3*-positive states along the pseudotime trajectory.

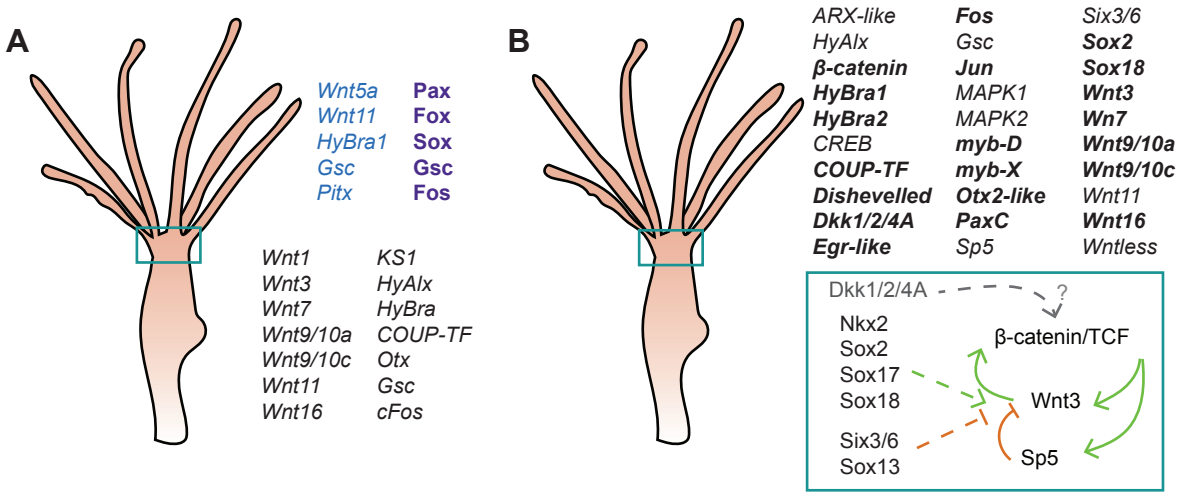

Figure 5. Head organizer genes and model of Wnt3/β-catenin signaling in *Hydra*. A) Previously predicted head organizer genes *Hydra*. In black is a list of genes previously found to be expressed in the *Hydra* hypostome using RNA-seq and *in situ* hybridization. In blue are genes with increased enhancer activity when Wnt signaling is activated. In purple is a list of transcription factors that show dynamic signatures of accessibility during regeneration. B) Top: Candidate regeneration genes expressed in head organizer cells, with *Wnt3* in pseudotime, or with *Wnt3* in the darkgreen module. In bold are genes that we found co-regulated with *Wnt3* using WGCNA and/or co-expressed with *Wnt3* in the same cell. Bottom: Proposed model of *Wnt3* signaling regulation. Solid lines represent known interactions and dashed lines represent predicted interactions based on pseudotime and ATAC-seq analysis. Green lines are positive, orange are negative, and gray are unknown but predicted interactions.

Supplemental Figures

Figure S1. Single cell RNA-seq sample distribution and clustering. A) Violin plot of nFeatures per sample. B). Violin plot of nCounts per sample. C) PCA plot of all samples. D) UMAP of cell clusters for the genome-level analysis.

Figure S2. Clustering and expression of genes used to determine distinct cell types. A) KS1. B) Dkk1/2/4A. C) SoxC. D) Nematogalectin. E) PaxA. F) MybX. G) Cnidocyte-specific; not annotated. H) KVamide. I) Teverse transcriptase. J) Jockey-like. K) Wnt3. L) Beta-catenin. M) Dishevelled. N) Sp5. O) Wntless.

Figure S3. Transcript-level clustering and expression. A) UMAP of transcript level seurat which gave 9 clusters 0-8. B) UMAP of predicted cell types using top differentially expressed genes and known cell markers. C) Expression of regeneration and developmental genes in the 9 clusters. D) Clustering and expression of Wnt3. E) Subclustering of Cluster 6, the epithelial progenitor-like cells. F) Expression of Wnt signaling genes in subclusters of cluster 6 reveal candidate head organizer cells.

Figure S4. Heatmap of top markers for clusters 0-8 at the transcript-level.

Figure S5. Clustering and expression of Wnt and Wnt signaling genes.

Supplemental Items:

Figure S6. Summary of candidate gene expression in different cell types.

Figure S7. *Fox* family genes clustering and expression.

Figure S8. *Sox* family genes clustering and expression.

Figure S9. WGCNA gene enrichment and correlations full. A) GO enrichment of darkgreen module. B) Go enrichment of coral2. C) Correlations for all modules against all cell types.

Figure S10. Expression of *Wnt3*-positive cells in pseudotime. A is transcript-level results; B and C are genome level results. A) Heatmap of candidate regeneration gene expression along pseudotime in states 1, 2, 4 and 5. B) Cells divide into 5 states, two of which are Wnt3+. C) State 1 includes mostly hypostome steady state cells while state 3 is mostly made up of t0 and t4 cells so we refer to this as the early regenerating head organizer.

Table S1. scRNA-seq statistics

Table S2. Top markers for head organizer cell clusters

Table S3. Gene list for darkgreen module

Table S4. Gene list for coral2 module

Table S5. Transcription factor binding for the *Wnt3* enhancer and promoter

References:

Alexa, A., and Rahnenfuhrer, J. topGO: Enrichment Analysis for Gene Ontology. R Packag. Version 2.46.0.

Aztekin, C., Hiscock, T.W., Marioni, J.C., Gurdon, J.B., Simons, B.D., and Jullien, J. (2019). Identification of a regeneration-organizing cell in the *Xenopus* tail. Science. *364*, 653–658. https://doi.org/10.1126/science.aav9996.

Babonis, L.S., and Martindale, M.Q. (2017). PaxA, but not PaxC, is required for cnidocyte development in the sea anemone *Nematostella vectensis*. Evodevo *8*, 1–20. https://doi.org/10.1186/s13227-017-0077-7.

Bentsen, M., Goymann, P., Schultheis, H., Klee, K., Petrova, A., Wiegandt, R., Fust, A., Preussner, J., Kuenne, C., Braun, T., et al. (2020). ATAC-seq footprinting unravels kinetics of transcription factor binding during zygotic genome activation. Nat. Commun. *11*. https://doi.org/10.1038/s41467-020-18035-1.

Bielen, H., Oberleitner, S., Marcellini, S., Gee, L., Lemaire, P., Bode, H.R., Rupp, R., and Technau, U. (2007). Divergent functions of two ancient *Hydra Brachyury* paralogues suggest specific roles for their C-terminal domains in tissue fate induction. Development *134*, 4187–4197. https://doi.org/10.1242/dev.010173.

Bode, H.R. (2003). Head regeneration in *Hydra*. Dev. Dyn. *226*, 225–236. https://doi.org/10.1002/dvdy.10225.

Bode, H.R. (2012). The head organizer in *Hydra*. Int. J. Dev. Biol. *56*, 473–478. https://doi.org/10.1387/ijdb.113448hb.

Boehm, A.M., Khalturin, K., Anton-Erxleben, F., Hemmrich, G., Klostermeier, U.C., Lopez-Quintero, J.A., Oberg, H.H., Puchert, M., Rosenstiel, P., Wittlieb, J., et al. (2012). FoxO is a

critical regulator of stem cell maintenance in immortal *Hydra*. Proc. Natl. Acad. Sci. *109*, 19697–19702. https://doi.org/10.1073/pnas.1221369110.

Bolger, A.M., Lohse, M., and Usadel, B. (2014). Trimmomatic: A flexible trimmer for Illumina sequence data. Bioinformatics *30*, 2114–2120. https://doi.org/10.1093/bioinformatics/btu170.

Bourque, G. (2009). Transposable elements in gene regulation and in the evolution of vertebrate genomes. Curr. Opin. Genet. Dev. *19*, 607–612. https://doi.org/10.1016/j.gde.2009.10.013.

Bray, N.L., Pimentel, H., Melsted, P., and Pachter, L. (2016). Near-optimal probabilistic RNA-seq quantification. Nat. Biotechnol. *34*, 525–527. https://doi.org/10.1038/nbt.3519.

Broun, M., and Bode, H.R. (2002). Characterization of the head organizer in hydra. Development *129*, 875–884. .

Broun, M., Sokol, S., and Bode, H.R. (1999). *Cngsc*, a homologue of *goosecoid*, participates in the patterning of the head, and is expressed in the organizer region of *Hydra*. Development *126*, 5245–5254. .

Browne, E.N. (1909). The production of new hydranths in *Hydra* by the insertion of small grafts. J. Exp. Zool. *7*, 1–23. https://doi.org/10.1002/jez.1400070102.

Butler, A., Hoffman, P., Smibert, P., Papalexi, E., and Satija, R. (2018). Integrating single-cell transcriptomic data across different conditions, technologies, and species. Nat. Biotechnol. *36*, 411–420. https://doi.org/10.1038/nbt.4096.

Cazet, J., Cho, A., and Juliano, C. (2021). Generic injuries are sufficient to induce ectopic wnt organizers in *Hydra*. Elife *10*, 1–31. https://doi.org/10.7554/eLife.60562.

Chapman, J.A., Kirkness, E.F., Simakov, O., Hampson, S.E., Mitros, T., Weinmaier, T., Rattei, T., Balasubramanian, P.G., Borman, J., Busam, D., et al. (2010). The dynamic genome of *Hydra*. Nature *464*, 592–596. https://doi.org/10.1038/nature08830.

Chari, T., Weissbourd, B., Gehring, J., Ferraioli, A., Leclère, L., Herl, M., Gao, F., Chevalier, S., Copley, R.R., Houliston, E., et al. (2021). Whole Animal Multiplexed Single-Cell RNA-Seq Reveals Plasticity of *Clytia* Medusa Cell Types. BioRxiv 2021.01.22.427844. .

Clapes, T., Polyzou, A., Prater, P., Sagar, Morales-Hernández, A., Ferrarini, M.G., Kehrer, N., Lefkopoulos, S., Bergo, V., Hummel, B., et al. (2021). Chemotherapy-induced transposable elements activate MDA5 to enhance haematopoietic regeneration. Nat. Cell Biol. *23*, 704–717. https://doi.org/10.1038/s41556-021-00707-9.

Conesa, A., Götz, S., García-Gómez, J.M., Terol, J., Talón, M., and Robles, M. (2005). Blast2GO: A universal tool for annotation, visualization and analysis in functional genomics research. Bioinformatics *21*, 3674–3676. https://doi.org/10.1093/bioinformatics/bti610.

Diacou, R., Zhao, Y., Zheng, D., Cvekl, A., and Liu, W. (2018). Six3 and Six6 Are Jointly Required for the Maintenance of Multipotent Retinal Progenitors through Both Positive and Negative Regulation. Cell Rep. *25*, 2510-2523.e4. https://doi.org/10.1016/j.celrep.2018.10.106.

Endl, I., Lohmann, J.U., and Bosch, T.C.G. (1999). Head-specific gene expression in *Hydra*: Complexity of DNA-protein interactions at the promoter of *ks1* is inversely correlated to the head activation potential. Proc. Natl. Acad. Sci. U. S. A. *96*, 1445–1450. https://doi.org/10.1073/pnas.96.4.1445.

Fan, Y., Wang, S., Hernandez, J., Yenigun, V.B., Hertlein, G., Fogarty, C.E., Lindblad, J.L., and Bergmann, A. (2014). Genetic Models of Apoptosis-Induced Proliferation Decipher Activation of JNK and Identify a Requirement of EGFR Signaling for Tissue Regenerative Responses in *Drosophila*. PLoS Genet. *10*. https://doi.org/10.1371/journal.pgen.1004131.

Geng, Q., Deng, H., Fu, J., and Cui, F. (2020). SOX18 exerts tumor-suppressive functions in papillary thyroid carcinoma through inhibition of Wnt/β-catenin signaling. Exp. Cell Res. *396*,

112249. https://doi.org/10.1016/j.yexcr.2020.112249.

Gerber, T., Murawala, P., Knapp, D., Masselink, W., Schuez, M., Hermann, S., Gac-Santel, M., Nowoshilow, S., Kageyama, J., Khattak, S., et al. (2018). Single-cell analysis uncovers convergence of cell identities during axolotl limb regeneration. Science (80-.). *362*. https://doi.org/10.1126/science.aaq0681.

Gerdes, P., Richardson, S.R., Mager, D.L., and Faulkner, G.J. (2016). Transposable elements in the mammalian embryo: Pioneers surviving through stealth and service. Genome Biol. *17*, 1–17. https://doi.org/10.1186/s13059-016-0965-5.

Gierer, A., Berking, S., Bode, H., David, C.N., Flick, K., Hansmann, G., Schaller, H., and Trenkner, E. (1972). Regeneration of *Hydra* from reaggregated cells. Nature *239*, 98–101. https://doi.org/10.1038/239500a0.

Goldman, J.A., and Poss, K.D. (2020). Gene regulatory programmes of tissue regeneration. Nat. Rev. Genet. *21*, 511–525. https://doi.org/10.1038/s41576-020-0239-7.

Greber, M.J., David, C.N., and Holstein, T.W. (1992). A quantitative method for separation of living Hydra cells. Roux's Arch. Dev. Biol. *201*, 296–300. https://doi.org/10.1007/BF00592110.

Grogg, M.W., Call, M.K., Okamoto, M., Vergara, M.N., Del Rio-Tsonis, K., and Tsonis, P.A. (2005). BMP inhibition-driven regulation of six-3 underlies induction of newt lens regeneration. Nature *438*, 858–862. https://doi.org/10.1038/nature04175.

Guder, C., Pinho, S., Nacak, T.G., Schmidt, H.A., Hobmayer, B., Niehrs, C., and Holstein, T.W. (2006). An ancient Wnt-dickkopf antagonism in *Hydra*. Development *133*, 901–911. https://doi.org/10.1242/dev.02265.

Hackett, J.A., Kobayashi, T., Dietmann, S., and Surani, M.A. (2017). Activation of Lineage Regulators and Transposable Elements across a Pluripotent Spectrum. Stem Cell Reports *8*,

1645–1658. https://doi.org/10.1016/j.stemcr.2017.05.014.

Hobmayer, B., Rentzsch, F., Kuhn, K., Happel, C.M., Von Laue, C.C., Snyder, P., Rothbächer, U., and Holstein, T.W. (2000). WNT signalling molecules act in axis formation in the diploblastic metazoan *Hydra*. Nature *407*, 186–189. https://doi.org/10.1038/35025063.

Holstein, T.W., Mala, C., Kurz, E., Bauer, K., Greber, M., and David, C.N. (1992). The primitive metazoan Hydra expresses antistasin, a serine protease inhibitor of vertebrate blood coagulation: cDNA cloning, cellular localisation and developmental regulation. FEBS Lett. *309*, 288–292. https://doi.org/10.1016/0014-5793 (92)80791-E.

Kamp, K., Noguchi, K., and Senba, E. (1995). Cell & Tissue gene mRNAs in regenerating rat skeletal muscle. *5*, 11–19. .

Kopp, A. (2009). Metamodels and phylogenetic replication: A systematic approach to the evolution of developmental pathways. Evolution (N. Y). *63*, 2771–2789. https://doi.org/10.1111/j.1558-5646.2009.00761.x.

Kormish, J.D., Sinner, D., and Zorn, A.M. (2010). Interactions between SOX factors and Wnt/β-catenin signaling in development and disease. Dev. Dyn. *239*, 56–68. https://doi.org/10.1002/dvdy.22046.

Langfelder, P., and Horvath, S. (2008). WGCNA: An R package for weighted correlation network analysis. BMC Bioinformatics *9*. https://doi.org/10.1186/1471-2105-9-559.

Langmead, B., and Salzberg, S.L. (2012). Fast gapped-read alignment with Bowtie 2. Nat. Methods *9*, 357–359. https://doi.org/10.1038/nmeth.1923.

Lengfeld, T., Watanabe, H., Simakov, O., Lindgens, D., Gee, L., Law, L., Schmidt, H.A., Özbek, S., Bode, H., and Holstein, T.W. (2009). Multiple Wnts are involved in *Hydra* organizer formation and regeneration. Dev. Biol. *330*, 186–199.

https://doi.org/10.1016/j.ydbio.2009.02.004.

Li, H., and Durbin, R. (2009). Fast and accurate short read alignment with Burrows-Wheeler transform. Bioinformatics *25*, 1754–1760. https://doi.org/10.1093/bioinformatics/btp324.

Love, M.I., Huber, W., and Anders, S. (2014). Moderated estimation of fold change and dispersion for RNA-seq data with DESeq2. Genome Biol. *15*, 1–21. https://doi.org/10.1186/s13059-014-0550-8.

Low, Y., Tan, D.E.K., Hu, Z., Tan, S.Y.X., and Tee, W.W. (2021). Transposable Element Dynamics and Regulation during Zygotic Genome Activation in Mammalian Embryos and Embryonic Stem Cell Model Systems. Stem Cells Int. *2021*. https://doi.org/10.1155/2021/1624669.

Marfil, V., Moya, M., Pierreux, C.E., Castell, J. V., Lemaigre, F.P., Real, F.X., and Bort, R. (2010). Interaction between Hhex and SOX13 modulates Wnt/TCF activity. J. Biol. Chem. *285*, 5726–5737. https://doi.org/10.1074/jbc.M109.046649.

Mashanov, V.S., Zueva, O.R., and García-Arrarás, J.E. (2012). Posttraumatic regeneration involves differential expression of long terminal repeat (LTR) retrotransposons. Dev. Dyn. *241*, 1625–1636. https://doi.org/10.1002/dvdy.23844.

Miyoshi, H., Ajima, R., Luo, C.L., Yamaguchi, T.P., and Stappenbeck, T.S. (2012). Wnt5a potentiates TGF-β signaling to promote colonic crypt regeneration after tissue injury. Science (80-.). *338*, 108–113. .

Morello, D., Fitzgerald, M.J., Babinet, C., and Fausto, N. (1990). c-myc, c-fos, and c-jun regulation in the regenerating livers of normal and H-2K/c-myc transgenic mice. Mol. Cell. Biol. *10*, 3185–3193. https://doi.org/10.1128/mcb.10.6.3185.

Münder, S., Tischer, S., Grundhuber, M., Büchels, N., Bruckmeier, N., Eckert, S., Seefeldt, C.A.,

Prexl, A., Käsbauer, T., and Böttger, A. (2013). Notch-signalling is required for head regeneration and tentacle patterning in *Hydra*. Dev. Biol. *383*, 146–157. https://doi.org/10.1016/j.ydbio.2013.08.022.

Murad, R., Macias-Muñoz, A., Wong, A., Ma, X., and Mortazavi, A. (2021). Coordinated Gene Expression and Chromatin Regulation during Hydra Head Regeneration . Genome Biol. Evol. *13*, 1–17. https://doi.org/10.1093/gbe/evab221.

Nakamura, Y., Tsiairis, C.D., Özbek, S., and Holstein, T.W. (2011a). Autoregulatory and repressive inputs localize Hydra Wnt3 to the head organizer. Proc. Natl. Acad. Sci. U. S. A. *108*, 9137–9142. https://doi.org/10.1073/pnas.1018109108.

Nakamura, Y., Tsiairis, C.D., Ozbek, S., and Holstein, T.W. (2011b). Autoregulatory and repressive inputs localize Hydra Wnt3 to the head organizer. Proc. Natl. Acad. Sci. *108*, 9137–9142. https://doi.org/10.1073/pnas.1018109108.

Noda, K. (1971). Reconstitution of dissociated cells of *Hydra*. Zool. Mag. *80*, 99–101. .

Petersen, H.O., Höger, S.K., Looso, M., Lengfeld, T., Kuhn, A., Warnken, U., Nishimiya-Fujisawa, C., Schnölzer, M., Krüger, M., Özbek, S., et al. (2015). A comprehensive transcriptomic and proteomic analysis of hydra head regeneration. Mol. Biol. Evol. *32*, 1928–1947. https://doi.org/10.1093/molbev/msv079.

Philipp, I., Aufschnaiter, R., Ozbek, S., Pontasch, S., Jenewein, M., Watanabe, H., Rentzsch, F., Holstein, T.W., and Hobmayer, B. (2009). Wnt/β-Catenin and noncanonical Wnt signaling interact in tissue evagination in the simple eumetazoan *Hydra*. Proc. Natl. Acad. Sci. *106*, 4290–4295. .

Qiu, X., Mao, Q., Tang, Y., Wang, L., Chawla, R., Pliner, H.A., and Trapnell, C. (2017). Reversed graph embedding resolves complex single-cell trajectories. Nat. Methods *14*, 979–982.

https://doi.org/10.1038/nmeth.4402.

Ramirez, A.N., Loubet-Senear, K., and Srivastava, M. (2020). A Regulatory Program for Initiation of Wnt Signaling during Posterior Regeneration. Cell Rep. *32*, 108098. https://doi.org/10.1016/j.celrep.2020.108098.

Reddy, P.C., Gungi, A., Ubhe, S., Pradhan, S.J., Kolte, A., and Galande, S. (2019). Molecular signature of an ancient organizer regulated by Wnt/β-catenin signalling during primary body axis patterning in Hydra. Commun. Biol. *2*, 1–11. https://doi.org/10.1038/s42003-019-0680-3.

Reddy, P.C., Gungi, A., Ubhe, S., and Galande, S. (2020). Epigenomic landscape of enhancer elements during Hydra head organizer formation. Epigenetics and Chromatin *13*, 1–16. https://doi.org/10.1186/s13072-020-00364-6.

Romagnoli, D., Boccalini, G., Bonechi, M., Biagioni, C., Fassan, P., Bertorelli, R., Sanctis, V. De, Leo, A. Di, Migliaccio, I., Malorni, L., et al. (2018). DdSeeker: A tool for processing Bio-Rad ddSEQ single cell RNA-seq data. BMC Genomics *19*, 1–7. https://doi.org/10.1186/s12864-018-5249-x.

Sabin, K.Z., Jiang, P., Gearhart, M.D., Stewart, R., and Echeverri, K. (2019). AP-1cFos/JunB/miR-200a regulate the pro-regenerative glial cell response during axolotl spinal cord regeneration. Commun. Biol. *2*. https://doi.org/10.1038/s42003-019-0335-4.

Schaffer, A.A., Bazarsky, M., Levy, K., Chalifa-Caspi, V., and Gat, U. (2016). A transcriptional time-course analysis of oral vs. aboral whole-body regeneration in the Sea anemone Nematostella vectensis. BMC Genomics *17*, 1–22. https://doi.org/10.1186/s12864-016-3027-1.

Sebé-Pedrós, A., Saudemont, B., Chomsky, E., Plessier, F., Mailhé, M.P., Renno, J., Loe-Mie, Y., Lifshitz, A., Mukamel, Z., Schmutz, S., et al. (2018). Cnidarian Cell Type Diversity and Regulation Revealed by Whole-Organism Single-Cell RNA-Seq. Cell *173*, 1520-1534.e20.

https://doi.org/10.1016/j.cell.2018.05.019.

Siebert, S., Thomsen, S., Reimer, M.M., and Bosch, T.C.G. (2005). Control of foot differentiation in *Hydra*: Phylogenetic footprinting indicates interaction of head, bud and foot patterning systems. Mech. Dev. *122*, 998–1007. https://doi.org/10.1016/j.mod.2005.04.010.

Siebert, S., Farrell, J.A., Cazet, J.F., Abeykoon, Y.L., Primack, A.S., Schnitzler, C.E., and Juliano, C.E. (2019). Stem cell differentiation trajectories in *Hydra* resolved at single-cell resolution. Science. *365*, eaav9314. https://doi.org/10.1101/460154.

Sinigaglia, C., Busengdal, H., Leclère, L., Technau, U., and Rentzsch, F. (2013). The Bilaterian Head Patterning Gene six3/6 Controls Aboral Domain Development in a Cnidarian. PLoS Biol. *11*. https://doi.org/10.1371/journal.pbio.1001488.

Slotkin, R.K., and Martienssen, R. (2007). Transposable elements and the epigenetic regulation of the genome. Nat. Rev. Genet. *8*, 272–285. https://doi.org/10.1038/nrg2072.

Smith, K.M., Gee, L., and Bode, H.R. (2000). HyAlx, an aristaless-related gene, is involved in tentacle formation in *Hydra*. Development *127*, 4743–4752. .

Srivastava, M. (2021). Beyond Casual Resemblance: Rigorous Frameworks for Comparing Regeneration Across Species. Annu. Rev. Cell Dev. Biol. *37*, 415–440. https://doi.org/10.1146/annurev-cellbio-120319-114716.

Steele, R.E. (2012). The *Hydra* genome: insights, puzzles and opportunities for developmental biologists. Int. J. Dev. Biol. *56*, 535–542. https://doi.org/10.1387/ijdb.113462rs.

Stierwald, M., Yanze, N., Bamert, R.P., Kammermeier, L., and Schmid, V. (2004). The Sine oculis/Six class family of homeobox genes in jellyfish with and without eyes: Development and eye regeneration. Dev. Biol. *274*, 70–81. https://doi.org/10.1016/j.ydbio.2004.06.018.

Stuart, T., Butler, A., Hoffman, P., Hafemeister, C., Papalexi, E., Mauck, W.M., Hao, Y.,

Stoeckius, M., Smibert, P., and Satija, R. (2019). Comprehensive Integration of Single-Cell Data. Cell *177*, 1888-1902.e21. https://doi.org/10.1016/j.cell.2019.05.031.

Technau, U., and Bode, H.R. (1999). *HyBra1*, a Brachyury homologue, acts during head formation in *Hydra*. Development *126*, 999–1010. https://doi.org/10.1242/dev.126.5.999.

Technau, U., Cramer von Laue, C., Rentzsch, F., Luft, S., Hobmayer, B., Bode, H.R., and Holstein, T.W. (2000). Parameters of self-organization in *Hydra* aggregates. Proc. Natl. Acad. Sci. *97*, 12127–12131. https://doi.org/10.1073/pnas.97.22.12127.

Tewari, A.G., Owen, J.H., Petersen, C.P., Wagner, D.E., and Reddien, P.W. (2019). A small set of conserved genes, including *sp5* and *Hox*, are activated by Wnt signaling in the posterior of planarians and acoels.

Trembley, A. (1744). Mémoires pour servir à l'histoire d'une genre de polypes d'eau douce, à bras en forme de cornes. (Leiden: Jean & Herman Verbeek).

Vogg, M.C., Beccari, L., Iglesias Ollé, L., Rampon, C., Vriz, S., Perruchoud, C., Wenger, Y., and Galliot, B. (2019). An evolutionarily-conserved Wnt3/β-catenin/Sp5 feedback loop restricts head organizer activity in Hydra. Nat. Commun. *10*, 1–15. https://doi.org/10.1038/s41467-018-08242-2.

Weinziger, R., Salgado, L.M., David, C.N., and Bosch, T.C. (1994). Ks1, an epithelial cell-specific gene, responds to early signals of head formation in Hydra. Development *120*, 2511–2517. .

Wenemoser, D., Lapan, S.W., Wilkinson, A.W., Bell, G.W., and Reddien, P.W. (2012). A molecular wound response program associated with regeneration initiation in planarians. Genes Dev. *26*, 988–1002. https://doi.org/10.1101 /aad.187377.112.

Wenger, Y., Buzgariu, W., Reiter, S., and Galliot, B. (2014). Injury-induced immune responses

in *Hydra*. Semin. Immunol. *26*, 277–294. https://doi.org/10.1016/j.smim.2014.06.004.

Wenger, Y., Buzgariu, W., and Galliot, B. (2016). Loss of neurogenesis in *Hydra* leads to compensatory regulation of neurogenic and neurotransmission genes in epithelial cells. Philos. Trans. R. Soc. B Biol. Sci. *371*, 20150040. https://doi.org/10.1098/rstb.2015.0040.

Yin, H., Zhengzuo, S., Zhang, X., Du, Y., Qin, C., Liu, H., Dun, Y., Qi, W., Jin, C., Zhao, Y., et al. (2017). Overexpression of SOX18 promotes prostate cancer progression via the regulation of TCF1, c-Myc, cyclin D1 and MMP-7. Oncol. Rep. *37*, 1045–1051. https://doi.org/10.3892/or.2016.5288.

Zheng, M., Zueva, O., and Hinman, V.F. (2022). Regeneration of the larval sea star nervous system by wounding induced respecification to the sox2 lineage. Elife *11*, 1–23. https://doi.org/10.7554/eLife.72983.

Zorn, A.M., Barish, G.D., Williams, B.O., Lavender, P., Klymkowsky, M.W., and Varmus, H.E. (1999). Regulation of Wnt signaling by Sox proteins: XSox17α/β and XSox3 physically interact with β-catenin. Mol. Cell *4*, 487–498. https://doi.org/10.1016/S1097-2765 (00)80200-2.